ELSEVIER

Polymer 41 (2000) 4543–4547

polymer

Proton magnetic resonance imaging in hydrogels: volume phase transition in poly(*N*-isopropylacrylamide)

S. Ganapathy[a], P.R. Rajamohanan[a], M.V. Badiger[a], A.B. Mandhare[a], R.A. Mashelkar[b,1,*]

[a]*National Chemical Laboratory, Pune 411 008, India*
[b]*Council of Scientific and Industrial Research, Anusandhan Bhawan, 2 Rafi Marg, New Delhi 110 001, India*

Received 21 May 1999; received in revised form 21 July 1999; accepted 4 August 1999

Abstract

Proton Magnetic Resonance (PMR) Imaging has been used to study the volume-phase-transition in a thermoreversible gel. This is demonstrated in the LCST polymer poly(*N*-isopropylacrylamide), swollen in water. The volume-phase-transition is conveniently monitored through one-dimensional proton images. PMR images, derived from relaxation and diffusion weighted planar spin-echo experiments, provide insights on the hydration state of water and the motional state of polymer, in the fully swollen and collapsed states of the gel.

Keywords: Hydrogels; Poly(*N*-isopropylacrylamide); Proton magnetic resonance imaging

1. Introduction

Polymeric gels that respond to stimuli, such as temperature, electric field, pH etc. have found wide-ranging applications in superabsorption, controlled drug delivery, bioseparations and biomedical fields [1–6]. Temperature-induced volume-phase-transition is one example of how a gel responds to the imposition of a macroscopic perturbation, and such a phenomenon usually occurs in gels that exhibit lower critical solution temperature (LCST). This has been well studied in the water swollen poly(*N*-isopropylacrylamide) (PNIPAm) gel, which undergoes a thermo-reversible volume phase transition at 31–32°C [7].

Although modern NMR spectroscopic methods have been used in the studies on gels by our group [8–10], as well as other groups [11–15], including the LCST phenomenon in PNIPAm [16–21], most of the work reported so far have dealt with the measurement of proton relaxation times (T_1,T_2) and self-diffusion coefficient of water (D_{self}) above and below the transition temperature. However, MRI has not been used to progressively monitor the LCST phenomenon in PNIPAm gel. Imaging experiments have been used earlier to monitor the solvent penetration profiles in rubbery and glassy polymers [13,22–26] and in the study of strained elastomers [27,28]. Similarly, magnetic resonance imaging (MRI) has been used in a recent study to image, in situ, the penetration of water in poly(ethylene oxide) [29]. Polymeric gels under equilibrium swollen conditions do not exhibit macroscopic spatial heterogeneity due to the intricate molecular level mixing of polymer and water domains, and, naturally, they would appear to discount the use of MRI for a study. However, it has been shown very recently that MRI can provide valuable information about the molecular motion of water in the collapsed PNIPAm gel [30]. In this paper, we have sought to use proton MRI to study the stimuli (temperature) response in the PNIPAm gel by noting that the dynamical behavior of polymer and water components occur at different motional timescales. This has allowed us to exploit and use associated dynamical parameters such as spin–lattice (T_1) and spin–spin (T_2) relaxation times and self-diffusion coefficient (D_{self}) for an image weighting.

2. Experimental

The proton imaging experiments were performed on a Bruker MSL-300 FT-NMR spectrometer operating at the proton Larmor frequency of 300.13 MHz. The spectrometer is equipped with a Bruker Micro-imaging unit (40 G/cm) and a dedicated imaging probehead. An imaging insert of 15 mm was used. The image acquisition was carried out

* Corresponding author. Tel.: +91-11-371-0472; fax: +91-11-371-0618.
E-mail address: csirhq@siynetd.ernet.in (R.A. Mashelkar).
[1] Director General, CSIR, and Secretary, Department of Scientific and Industrial Research.

0032-3861/00/$ - see front matter
PII: S0032-3861(99)00615-1

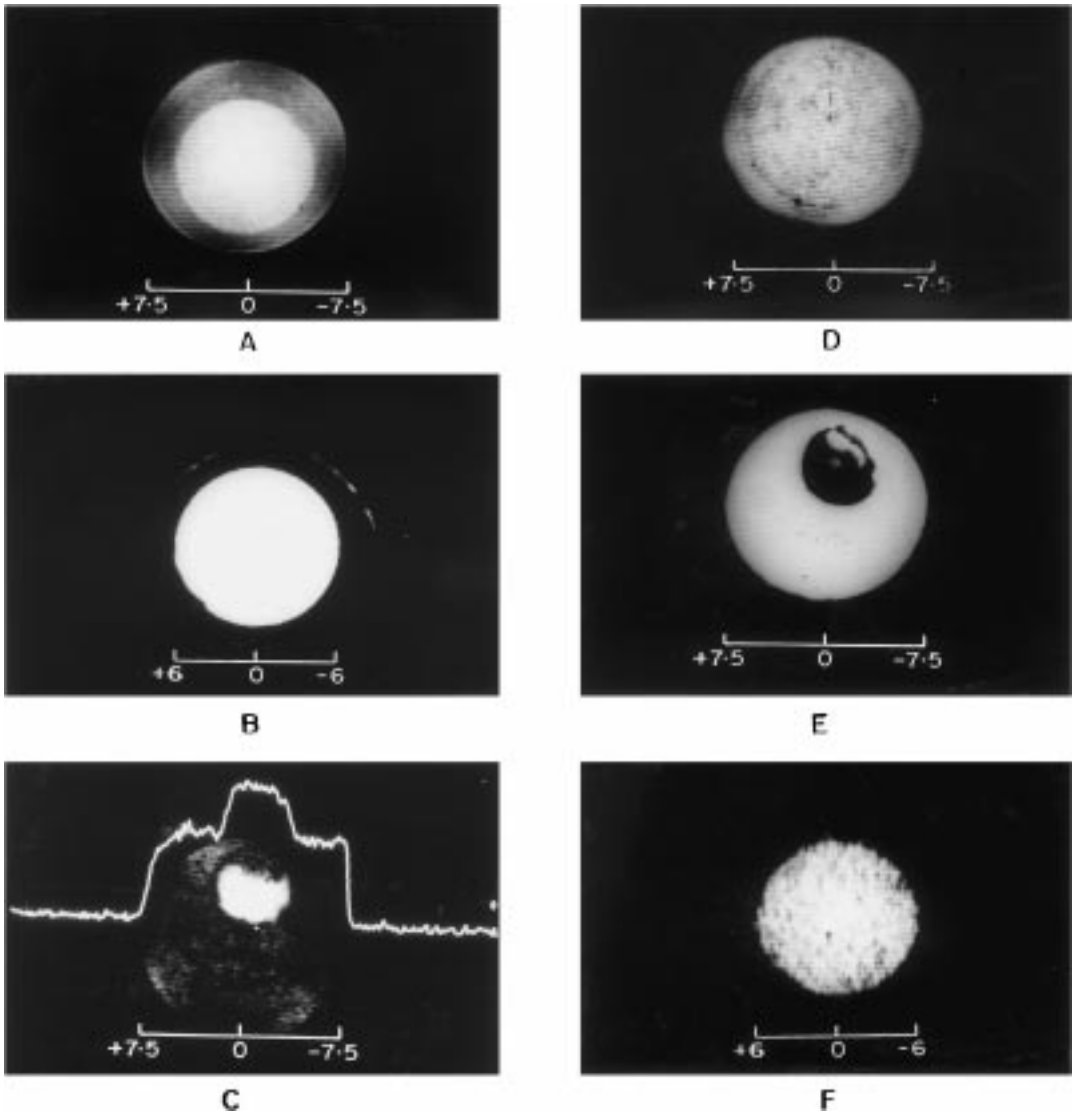

Fig. 1. Planar (*XY*) images obtained on equilibrium swollen: (A),(B),(D), and (F); and collapsed gel of poly(*N*-isopropyl acrylamide) (C), (E) at 22 and 40°C, respectively. (A),(B),(C): T_1 weighting; (D),(E): T_2 weighting and (F): Diffusion weighting. The T_1 weighting was achieved by adjusting the recycle delay to 2 s (A) and 750 ms (C), while in (B) the T_1 weighting is done by using an inversion recovery sequence prior to the slice selection and adjusting the τ delay (1.68 s) to null the water magnetization. The T_2 weighting scheme (D),(E) used a CPMG sequence ($\tau = 1$ ms for (D) and 50 ms for (E)) prior to the 2D imaging sequence. The diffusion weighting (F) was achieved by tailoring a PFG-SE sequence ($\delta = 5$ ms; $\Delta = 15$ ms; $G_Z = 22$ G/cm) prior to the 2D imaging sequence. The image in (E) is taken at a higher vertical scale due to poor *S*/*N*. The 1D proton spin density profile of the row passing through the center of the collapsed gel is also shown in (C). The length scale (in mm) along the radial direction is shown in the images.

using a standard spin-echo technique [31]. A sinc shaped r.f. pulse in the presence of *z*-gradient was used for slice (1 mm) selection. For the acquisition of one-dimensional proton spin density profiles of a chosen slice, the phase encoding was switched off and the spin-echo experiment conducted by varying the read gradient only. The spin system was preconditioned for relaxation (T_1,T_2) and diffusion (D_{self}) weighting by incorporating the appropriate pulse schemes, prior to slice selection, as explained in the respective figure captions. The temperature of the gel was precisely controlled using a Bruker BVT-1000 controller. PNIPAm was synthesized by polymerizing *N*-isopropylacrylamide monomer using ethylene glycol dimethacrylate as a cross-linking agent and azo-bis isobutyronitrile as an initiator [32].

3. Results and discussion

We show in Fig. 1 the comparison of planar proton images of PNIPAm gel in its equilibrium swollen state (22°C, below LCST,) and collapsed state (40°C, above LCST). These images, as well as others, were obtained on a swollen gel cast as a uniform cylinder of diameter 12 mm and centrally positioned in a glass tube (15 mm outer diameter) containing water. The collapse of the gel is

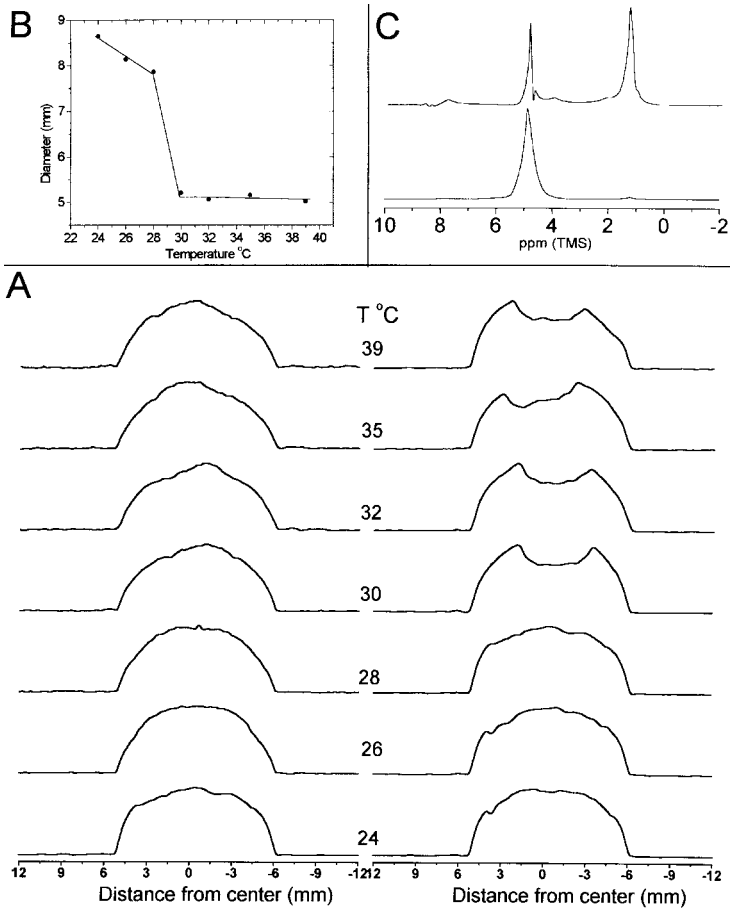

Fig. 2. (A) Proton spin density profiles of a slice (1 mm thickness) along the *X*-axis as a function of temperature in poly(*N*-isopropylacrylamide) gel, obtained with partial T_1 weighting (left, using fast recycle time of 750 ms) and with T_2 weighting (right). The pulse scheme consists of the usual CPMG sequence (τ delay of 50 ms), prior to the slice selection using a sinc shaped soft π pulse, with the phase encoding switched off during the 1D imaging. The spin system is preconditioned with the decay of the transverse magnetization during the τ delay period to produce an effective T_2 weighting on the 1D-image profiles. The 1D image profiles were obtained by Fourier transformation of the echo, followed by magnitude calculation. (B) A plot depicting the LCST transition from the T_2 weighted 1D image profile data. (C) Normal 1D ^{1}H spectrum of the gel with (top) and without (bottom) water suppression. The water suppression was achieved by selectively dephasing the transverse magnetization of water through its fast self-diffusion ($D_{self} = 2.2 \times 10^{-5}$ cm^2/s) [32]. The enhanced signal resolution for the proton resonances in the repeat unit of the polymer may be seen in the bottom spectrum.

noticed as decreased circular cross-sectional area (Fig. 1). The LCST transition is more precisely depicted through one-dimensional images, as demonstrated in Fig. 2. Since the applied gradient varies linearly, the projection of proton signal intensity from the excited slice of a cylindrical gel is semi-circular (Fig. 2A, left). However, to distinctly monitor the LCST transition of PNIPAm gel, we have used a T_2 weighting scheme at the beginning of the pulse sequence to distinguish the one-dimensional image profile due to polymeric gel in the middle (Fig. 2A, right) from the overall profile (Fig. 2A, right). This aids in the clear depiction of the volume phase transition in PNIPAm (Fig. 2B). Further, the imaging experiments show that PNIPAm behaves as a conventional isotropic gel [33] so that for a cylindrically shaped gel the swelling ratios in the axial and radial directions are the same after the thermal collapse.

Further insights into the state of water in the gel as well as the enhanced molecular mobility of the polymer are provided in the relaxation (T_1,T_2) and diffusion (D_{self}) weighted proton images presented in Fig. 1. The enhanced polymer mobility is reflected from the large signal amplitude for the polymer protons of the gel structure when a T_1 weighting is employed prior to image acquisition. The polymer contribution to the gel image is emphasized (Fig. 1B) by tailoring an inversion recovery scheme prior to the imaging sequence and adjusting the τ delay to put the water at its relaxation null. This may be compared with the image obtained in the absence of any T_1 preconditioning (Fig. 1A). For the water in the polymer, exchange is rapid among the bound and free states, characterized by their respective site populations P_b and P_f, and, further in the equilibrium swollen gel, $P_f \gg P_b$. The spin–lattice relaxation time, being a population weighted average of relaxation time for water in its bound (T_{1b}) and free (T_{1f}) states [34,35], therefore approaches that of bulk water in the equilibrium swollen gel. By the employed T_1 weighting scheme, we have nearly eliminated the contribution from water protons to the image, so that an exclusive contribution from polymer

protons to the image is emphasized in Fig. 1B. It may be noted that the T_1 weighting has little effect on the polymer protons since their spin–lattice relaxation times lie in the hundreds of msec range which are an order of magnitude smaller than the T_1 of water in the equilibrium swollen gel. The observation further shows that in the equilibrium swollen gel the homonuclear proton–proton dipolar interactions are effectively removed by hydration induced polymer motions so that the proton resonances of the polymer are exited by the pulse scheme and detected in the imaging experiment. This is supported by the fine proton resolution observable in the water suppressed ^{1}H spectrum (Fig. 2C) as well in our earlier magic angle spinning (MAS) experiments of PNIPAm gel [16,17]. The thermally induced collapse of the gel, depicting the volume phase transition, is clearly seen in the proton image and 1D profile shown in Fig. 1C.

The T_2 weighted images of the equilibrium swollen and collapsed PNIPAm gel are shown in Fig. 1D and E, respectively. For the equilibrium swollen gel (Fig. 1E), the proton density of exterior water, gel water and polymer protons all contribute to the image intensity, due to the short dephasing delay (1 ms) we have used, compared to the spin–spin relaxation time of water (ca 3 s) and that of polymer protons (10–20 ms). The thermal collapse of the gel, past the volume phase transition, is clearly depicted in the T_2 weighted image shown in Fig. 1E. The dramatically enhanced contrast between the exterior water in the tube and the collapsed gel can be achieved when a longer T_2 dephasing delay (50 ms) was deliberately used. The T_2 weighted image in Fig. 1E shows uneven proton spin density in a small region of the collapsed gel, possibly due to heterogeneous water release and or a thermal gradient across the gel. Interestingly, the same feature may also be noticed in the T_1 weighted image of the collapsed gel (Fig. 1C). The heterogeneous release of water from the gel is in line with the observations of a bicomponent proton T_2 decay in a collapsed gel, reported by Tanaka et al. [30].

The diffusional weighting in a gel also influences image contrast as shown in Fig. 1F. Here again, the exterior water that surrounds the gel has D_{self} of neat water and offers a benchmark for image comparison. In equilibrium swollen gel, D_{self} of water in the gel is governed by the diffusion of water in its bound and free states, appropriately weighted by their site populations and the associated self-diffusion coefficients [32]. In the equilibrium swollen state, where the free water content in the gel is high ($P_f = 0.95$), the difference in D_{self} of gel water and exterior water is not very large. Since polymer particles diffuse ever so slowly, a scheme which allows diffusional dephasing of water in the gel, and exterior water alike, would emphasize the contribution from the polymer component to the gel image. However, since the T_2 values for polymer protons are short (10–20 ms), there is a partial loss of polymer signal intensity in the diffusion weighted experiment due to an unavoidable T_2 dephasing in the spin-echo experiment. This would account for the poor S/N in Fig. 1F, quite in contrast to the T_1 weighting experiment in which the S/N for the polymer protons is inherently superior. We also tried to get a diffusion weighted image of the PNIPAm gel in its collapsed state (40°C) under identical experimental conditions. We however do not see any image at all. It may be realized that while the water contribution to the image intensity is nearly removed by the diffusional dephasing of the water magnetization, the polymer contribution is altogether absent due to the predominance of proton–proton dipolar interactions ($\Delta\nu_{dipolar} = 8$ kHz) in the collapsed state of the gel [17].

4. Conclusions

We have shown that proton-imaging experiments are viable in studying the stimuli response of polymeric gels. This has been demonstrated in the LCST polymer PNIPAm. Although the microscopic differences in the motional state of the polymer and water components are used to bring in image contrast through appropriate relaxation and diffusion weighting. In view of the adequate signal resolution for the polymer and water components, chemical shift based imaging experiments would be useful. These and other imaging experiments to determine water distribution in gels are under way.

References

[1] Dagani R. Chem Engng News 1997;75:26.
[2] DeRossi D, Kajiwara K, Osada Y, Yamauchi A, editors. Polymer gels: fundamental and biomedical applications New York: Plenum Press, 1991.
[3] Harland RS, Prud'homme RK, editors. Polyelectrolyte gels: properties, preparatios and applications ACS symposium series, 1992. pp. 480.
[4] Dušek K, editor. Responsive gels: volume transitions 1 & 2 Advances in polymer science, 109, 110. Berlin: Springer, 1993.
[5] Hoffman AS. Macromol Symp 1995;98:645.
[6] Dong LC, Hoffman AS. In: Russo PS, editor. Reversible polymeric gels and related systems, ACS symposium series, 350. , 1987. pp. 236.
[7] Schild HG. Prog Polym Sci 1992;17:163.
[8] Ganapathy S, Rajamohanan PR, Badiger MV, Mashelkar RA. . New Polym Mater 1990;2:205.
[9] Rajamohanan PR, Ganapathy S, Ray SS, Badiger MV, Mashelkar RA. Macromolecules 1995;28:2533.
[10] Ganapathy S, Badiger MV, Rajamohanan PR, Mashelkar RA. Macromolecules 1992;25:4255.
[11] Cohen Addad JP. Prog NMR Spectroscopy 1993;25:1.
[12] Yokota K, Abe A, Hosaka S, Sakai I, Saito H. Macromolecules 1978;11:95.
[13] Yasunaga H, Kobayashi M, Matsukawa S, Kurosu H, Ando I. Annual reports in NMR spectroscopy 1997;34:39.
[14] Pop IE, Dhalluin CF, Deprez BP, Melnyk PC, Lippens GM, Tartar AL. Tetrahedron 1996;52:12209.
[15] Gladden LF. Chem Engng Sci 1994;49:3339.
[16] Badiger MV, Kulkarni MG, Rajamohanan PR, Mashelkar RA. Macromolecules 1991;24:106.
[17] Ganapathy S, Rajamohanan PR, Ray SS, Mandhare AB, Mashelkar RA. Macromolecules 1994;27:3432.

[18] Tokuhiro T, Amiya T, Mamada A, Tanaka T. Macromolecules 1991;24:2936.
[19] Ohta H, Ando I, Fijishige S, Kubota K. J Mol Struct 1991;245:391.
[20] Ohta H, Ando I, Fujishige S, Kubota K. J Polym Sci Part B: Polym Phys 1991;29:963.
[21] Gibbs SJ, Johnson Jr. CS. Macromolecules 1991;24:6110.
[22] Koenig JL. In: Mathias LJ, editor. Solid state NMR of polymers, New York: Plenum Press, 1991 p. 61.
[23] Blümich B, Blümler P. Makromol Chem 1993;194:2133.
[24] Parker DD, Koenig JL. Current trends in polymer science 1996;1:65.
[25] Webb AG, Hall LD. Polymer 1991;32:2926.
[26] Hyde TM, Gladden LF, Mackley MR, Gao PJ. Polymer Sci Polym Chem Ed 1995;33:1795.
[27] Blumer P, Blümich B. Rubber Chem Technol 1997;70:468.
[28] Smith SR, Koenig JL. Macromolecules 1991;24:3496.
[29] Hyde TM, Gladden LF. Polymer 1998;39:811.
[30] Tanaka N, Matsukawa S, Kurosu H, Ando I. Polymer 1998;39: 4703.
[31] Callaghan PT. Principles of nuclear magnetic resonance microscopy, Oxford: Oxford University Press, 1991.
[32] Ray SS, Rajamohanan PR, Badiger MV, Devotta I, Ganapathy S, Mashelkar RA. Chem Engng Sci 1998;53:869.
[33] Li Y, Tanaka T. Polymer gel, New York: Plenum Press, 1991.
[34] Halle B, Wennerstrom H. J Chem Phys 1981;75:1928.
[35] Ganapathy S, Ray SS, Rajamohanan PR, Mashelkar RA. J Chem Phys 1995;103:6783.